

Power-Combined Rectenna Array for X-Band Wireless Power Transfer

Eric Kwiatkowski^{#1}, Christopher T. Rodenbeck^{\$2}, Taylor Barton^{#3}, Zoya Popovic^{#4}

[#]University of Colorado Boulder, Boulder, CO 80309 USA

^{\$}Naval Research Laboratory, Washington, DC 20375 USA

¹eric.kwiatkowski@colorado.edu, ²christopher.rodenbeck@nrl.navy.mil ³taylor.w.barton@colorado.edu, ⁴zoya@colorado.edu

Abstract—This work presents an RF power-combined rectenna array operating at 10 GHz and designed for low incident power densities ranging from 0.1-100 $\mu\text{W}/\text{cm}^2$. The array consists of unit-cell sequentially-fed four-element patch antenna subarrays designed to receive incident waves with circular polarization. The incident power is converted to dc using a single-ended Schottky diode rectifier. The rectifier is first characterized over input power and dc load individually and with a single sub-array. A 4-to-1 RF power-combining network is designed to further improve RF-to-dc conversion efficiency and output power at the lower-bound power density of 0.1 $\mu\text{W}/\text{cm}^2$. A three-layer PCB with off-the-shelf components enables straightforward scaling to larger apertures.

Keywords—wireless power transfer, rectenna, rectifying circuit, power combining, energy harvesting.

I. INTRODUCTION

Rectenna arrays for low incident power densities were first demonstrated in [1] at 2.45 GHz with 48 linearly-polarized antenna elements feeding a single 50- Ω matched rectifier. This array was tested with 5 $\mu\text{W}/\text{cm}^2$ incident power density with an efficiency on the order of 50% for a broadside incident wave. For harvesting applications (<100 $\mu\text{W}/\text{cm}^2$ power density), a number of rectennas were demonstrated and are reviewed in [2], with some examples of circularly polarized rectennas given in [3], [4]. Arrays of rectennas for harvesting, where each antenna element is loaded with a rectifier, are demonstrated primarily with isotropic power reception in mind. A broadband spiral dual-circularly polarized array was characterized down to incident power levels of 0.05 $\mu\text{W}/\text{cm}^2$ [5].

Here we present a 10-GHz left-hand circularly polarized (LHCP) rectenna array intended for extremely low power density reception, from 0.1-100 $\mu\text{W}/\text{cm}^2$, targeting space-to-Earth wireless power transfer applications. Commercially available diodes and standard PCB design techniques are selected to enable straightforward manufacturing and scaling to larger apertures. To address the challenges associated with this extremely low incident power, we first characterize the diode rectifier conversion efficiency over RF source impedance, RF input power and dc load resistance. A sub-array unit cell is then designed and power-combined as a 2×2 array feeding a single rectifier, as shown in the block diagram in Fig. 1. The unit cell and array are characterized over power, frequency, and elevation angle, demonstrating a measured broadside RF-dc conversion efficiency of 15% at 100 $\mu\text{W}/\text{cm}^2$ incident power density.

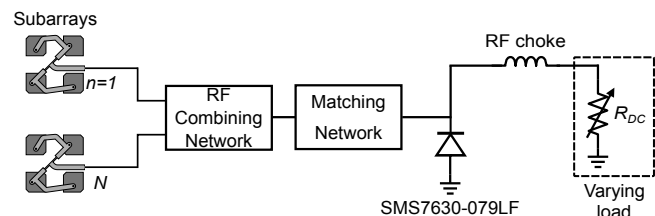


Fig. 1. Block diagram of RF power-combined rectenna array for N subarrays. In this paper, we demonstrate an array with $N = 4$ and each subarray is a LHCP sequentially-fed 4-element patch array.

II. RECTENNA UNIT CELL

The rectenna unit cell consists of a sequentially-fed array operating as an LHCP antenna, impedance matched to a single rectifying diode, with an RF choke providing a dc output. The rectifier and array are first characterized independently before being integrated into the array (Section III).

A. Design of Rectifier and Matching Network

Prior to integrating a diode rectifier into the patch array, a standalone matching network was designed to validate simulated and experimental source-pull results for a Skyworks SMS7630-079LF Schottky diode with package parasitics provided in [6] for an SOD523 package. Although smaller packages are commercially available (e.g., 0402 and 0201 SMT packages), the larger package is chosen due to its ease of attachment and repeatability in terms of measured performance across multiple diodes.

The matching network is designed to present $Z_{src} = 8 + j13.5 \Omega$ at the diode plane, equivalent to the source impedance obtained from source-pull simulations conducted with -30 to -10 dBm available source power. A simple matching network consisting of a 50- Ω 50° shunt stub and 50- Ω $\lambda_g/4$ line with a 0.3 pF shunt capacitor matches the diode impedance to 50 Ω . The dc output power is measured across a variable resistive load placed in parallel with the capacitor. Measured RF-dc conversion efficiency for varying input power levels and dc loads swept from 300 to 3 k Ω is shown in Fig. 2, along with the expected efficiency based on source-pull measurements. The dc load that results in the highest efficiency varies with incident power on the diode, and the value of the load is chosen as a compromise over the expected power levels. It can be observed that the magnitude of diode conversion efficiency exhibits greater variation as a function of dc load at higher power levels. Note that the targeted power density of 0.1

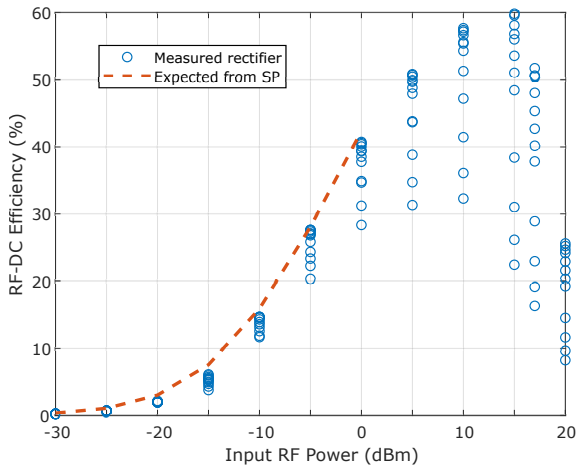


Fig. 2. Measured RF-dc conversion efficiency of single-diode rectifier matched to $Z_{src} = 8 + j13.5\Omega$ at 10 GHz. Each measured data point corresponds to a different dc load, with a range from 300 to 3 k Ω .

to 100 $\mu\text{W}/\text{cm}^2$ with an array size of the order of 10 cm^2 (about λ_0^2 at 10 GHz) results in expected power levels at a well-matched diode of -30 to 0 dBm.

B. Sequentially-Fed Array Design

In order to increase received RF power for a range of incidence angles and low incident power density, we increase the aperture size using a 2×2 planar array of patch antennas. The square patch elements are coaxially fed at an offset position that helps the match to a 50- Ω impedance, with notches on the corners that result in left-hand circular polarization (LHCP). The element gain is approximately 6 dB at a center frequency of 10 GHz. The feed network for the 2×2 array sequentially excites the elements with progressive phase shifts to further improve the axial ratio [7]. The simulated axial ratio at broadside of the unit cell sub-array is 0.7 dB at 10 GHz.

The radiating elements are fabricated on a RO3003 substrate ($\epsilon_r = 3.00$, $h = 30$ mil) with RO4450F prepreg ($\epsilon_r = 3.52$, $h = 4$ mil). The feed and subsequent combining and matching networks are fabricated on an identical RO3003 dielectric without a prepreg layer. A plasma/sodium etching process is required for proper via plating in ceramic-filled PTFE composites such as RO3003 [8].

The layout of a single unit cell incorporating the patch elements, sequential feed network, and matching network is shown in Fig. 3. A darker color is used for the patch elements to distinguish them from the rest of the design which is fabricated on a different layer of the stackup. The diode matching network is identical to that used to characterize the single rectifier in Fig. 2, and is shown in Fig. 3 at right.

III. POWER-COMBINED RECTENNA ARRAY

The power-combined rectenna array incorporates four subarrays ($N = 4$ in Fig. 1) in an effort to increase RF power rectified by a single diode. Because the rectifier efficiency increases nonlinearly with input power, system efficiency can

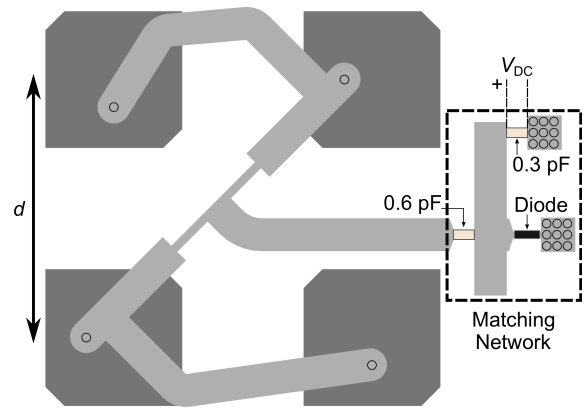


Fig. 3. Schematic of unit cell with validated matching network. Patch elements (darker) are located on top layer, feed and matching network (lighter) are on bottom layer. The center-to-center element spacing, d , is $\lambda_0/2$.

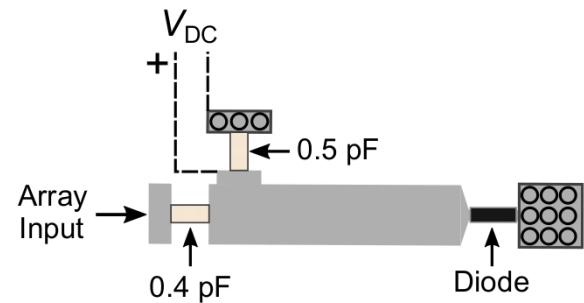


Fig. 4. Redesigned matching network for the 4-to-1 combined array.

be increased by collecting more input power for a single rectifier even in the presence of combining network losses. For example, utilizing simulated gain data of the four subarrays and a nonlinear rectifier efficiency model, the rectified output power of the array is calculated to be greater than that of a unit cell, as long as the combiner insertion loss is kept below 3 dB. Physical constraints limit how many subarrays can be power-combined in a planar layout while maintaining symmetry. Therefore, for this work a 2×2 array is used, with the dc output taken at the center of the array. An additional constraint is the high directivity that the array would have in a given direction, requiring mechanical steering to track the satellite transmitter.

To initially combine the subarrays at a location near the geometric center of the array, a tapered tee combiner was used with a characteristic impedance transition from 50 Ω to 35 Ω . Although the resulting input impedance at this point was approximately the same as that of the unit cell without a matching network, a revised smaller matching network needed to be designed due to size constraints. Fig. 4 shows the redesigned rectifier matching network. Vias are modeled in a full-wave simulator to account for parasitic inductance which is then compensated for in the network. The power-combined rectenna array, shown in Fig. 5, is approximately 6 \times 6 cm in size with a simulated axial ratio of 2 dB at broadside.

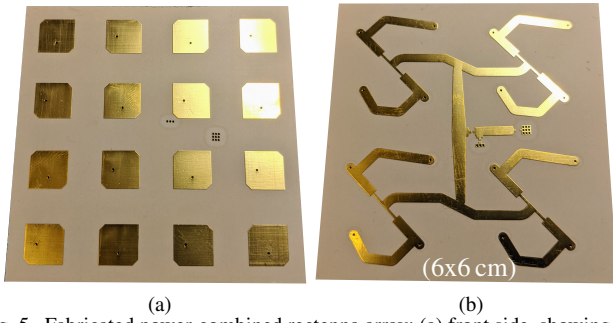


Fig. 5. Fabricated power-combined rectenna array: (a) front side, showing four unit cells with a total of sixteen patch elements; and (b) back side, including combining network and diode rectifier matching network (unpopulated).



Fig. 6. Photograph showing test setup for measuring rectenna arrays. An RF power source, variable dc load, and voltmeter are kept outside of the anechoic chamber.

IV. MEASURED PERFORMANCE

A photograph of the experimental setup is shown in Fig. 6. The distance between the co-polarized LHCP transmitting antenna and the rectenna array is maintained at 75 cm in order to ensure far-field conditions. A power meter, variable dc load, characterized RF power source with driver amplifier, and voltmeter were kept outside of the anechoic chamber to minimize possible electromagnetic interference. This setup measures both unit cell gain as well as unit cell and array rectenna output power and conversion efficiency. Conversion efficiency is a function of incidence angle and here defined as:

$$\eta = \frac{P_{dc}}{S_{inc}(\theta, \phi) \cdot A_{eff}(\theta, \phi)}. \quad (1)$$

where $S_{inc}(\theta, \phi)$ is the incident power density (in $\mu\text{W}/\text{cm}^2$) and $A_{eff}(\theta, \phi)$ is the effective area of the aperture in a given direction. For the unit cell, A_{eff} is calculated knowing the fixed ratio of gain to effective aperture at a single frequency at broadside. Since the gain of the combined rectenna array cannot be independently measured, its geometric area is used in place of the effective area at broadside, thus providing a conservative estimate for total conversion efficiency.

A. Unit Cell Measurements

Measurements of LHCP antenna gain (IEEE) and input match of the passive unit cell sub-array without integrated matching network are provided in Fig. 7. A TRL fixture is used to de-embed the effects of the connector. The unit cell exhibits a gain of approximately 9.8 dB at 10 GHz and return loss greater than 10 dB over a 1-GHz bandwidth.

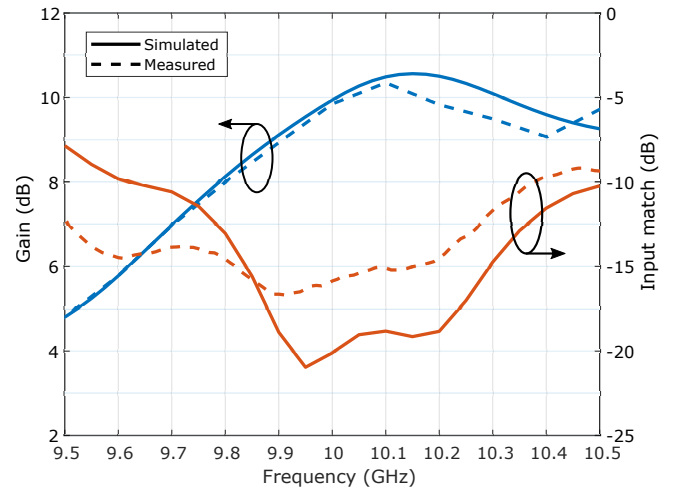


Fig. 7. Measured and simulated gain (IEEE) and input match for a passive unit cell sub-array without matching network. The input match is de-embedded via TRL calibration.

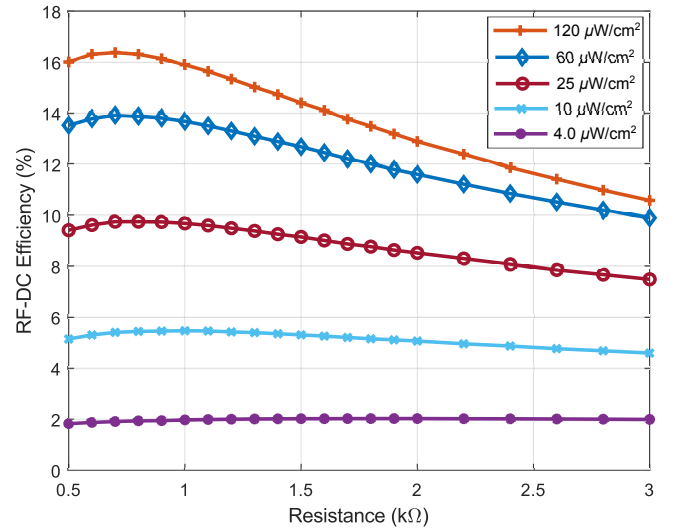


Fig. 8. Measured unit cell RF-dc conversion efficiency for varying loads and input power densities at 10 GHz and broadside incidence.

To examine the effect of the dc load on rectenna performance, a variable load is swept from 500 to 3 k Ω while simultaneously varying incident power density from 0.1 $\mu\text{W}/\text{cm}^2$ to 130 $\mu\text{W}/\text{cm}^2$ at 10 GHz. While a maximum conversion efficiency slightly above 16% is measured for a dc load of 750 Ω at maximum power density (as seen in Fig. 8), the ideal dc load is shown to increase towards, or exceed, 3 k Ω for decreasing power densities.

B. Power-Combined Array

Performance of the power-combined rectenna array was characterized in a similar manner to that of the unit cell, with incident power density swept over a 30-dB dynamic range at a fixed frequency and for varying dc loads. Fig. 9 shows output dc power (in dBm) and RF-dc conversion efficiency as a function of incident power density for both the unit cell and array. The conversion efficiencies shown here are taken as the

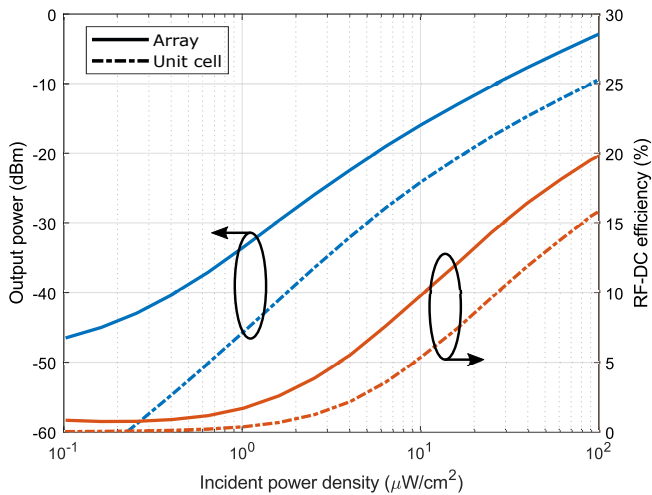


Fig. 9. Measured broadside RF-dc conversion efficiency and P_{dc} of unit cell and power-combined array at 10GHz. The efficiency is calculated using (1) and areas of the unit cell and array of 9 and 36 cm^2 , respectively.

peak value for a specified power density, which is dependent on dc load as exemplified in Fig. 8.

The combined array shows an increase in conversion efficiency over that of the unit cell for all power densities. Maximum efficiency for the combined array approaches 20% for a $100 \mu\text{W}/\text{cm}^2$ incident power density. A non-zero conversion efficiency at very low power densities for the array is due to an uncontrolled external source. The benefit of power-combining to a single diode is best seen by inspection of rectified dc power over the full range of incident power density. At $100 \mu\text{W}/\text{cm}^2$, the array produces above -5 dBm of dc power compared to the unit cell's output of -10 dBm, or a 5-dB relative increase in output power. At the lower-bound power density, this relative increase exceeds 10 dB.

Fig. 10 shows a relative comparison in dc output power for angles of incidence up to 30° off broadside for both the array and unit cell. While the benefit of power combining for broadside incidence is apparent, the combined array exhibits a narrower beamwidth compared to that of the unit cell thus producing lower rectified output power at larger angles of incidence.

V. CONCLUSION

This work presents a power-combined rectenna array and unit cell operating at 10 GHz for space-to-Earth wireless power transfer applications. An RF combining network is utilized to increase incident power on a single Schottky diode for the purpose of increasing conversion efficiency and dc output power for incident power densities as low as $0.1 \mu\text{W}/\text{cm}^2$. An increase in output power exceeding 10 dB relative to a non-power combined unit cell is demonstrated, showing potential for scaling to larger aperture sizes.

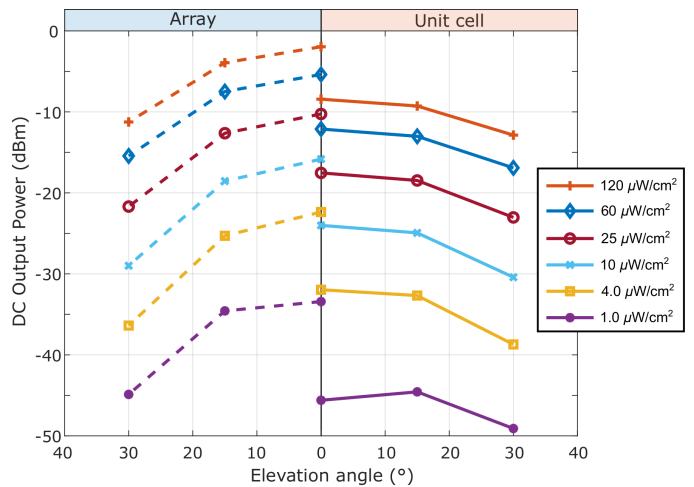


Fig. 10. Output dc power as a function of elevation angle for various power densities, measured for both the array and unit cell.

ACKNOWLEDGMENT

This work was funded by the Naval Research Laboratory under a contract with Envisioneering 19-02-0131-V101. Z. Popovic thanks Lockheed Martin for support from the Endowed Chair for RF Engineering. Modelithics models utilized under the University License Program from Modelithics, Inc., Tampa, FL, were used in designing the matching networks used in this work. The authors would like to thank M. Robinson for thoughtful discussion regarding feed network design.

REFERENCES

- [1] W. C. Brown, "An experimental low power density rectenna," in *1991 IEEE MTT-S International Microwave Symposium Digest*, July 1991, pp. 197–200 vol.1.
- [2] C. R. Valenta and G. D. Durgin, "Harvesting wireless power: Survey of energy-harvester conversion efficiency in far-field, wireless power transfer systems," *IEEE Microw. Mag.*, vol. 15, no. 4, pp. 108–120, June 2014.
- [3] Young-Ho Suh, Chunlei Wang, and Kai Chang, "Circularly polarised truncated-corner square patch microstrip rectenna for wireless power transmission," *Electronics Letters*, vol. 36, no. 7, pp. 600–602, March 2000.
- [4] B. Strassner and Kai Chang, "5.8-GHz circularly polarized dual-rhombic-loop traveling-wave rectifying antenna for low power-density wireless power transmission applications," *IEEE Trans. Microw. Theory Techn.*, vol. 51, no. 5, pp. 1548–1553, May 2003.
- [5] J. A. Hagerty, F. B. Helmbrecht, W. H. McCalpin, R. Zane, and Z. B. Popovic, "Recycling ambient microwave energy with broad-band rectenna arrays," *IEEE Transactions on Microwave Theory and Techniques*, vol. 52, no. 3, pp. 1014–1024, March 2004.
- [6] Avago, "Application note 1124: Linear models for diode surface mount packages," 2007, original document from Avago Technologies. [Online]. Available: https://docs.broadcom.com/wcs-public/products/application-notes/application-note/829/290/av02-0038en-an_1124-21jul10.pdf
- [7] P. S. Hall, J. S. Dahele, and J. R. James, "Design principles of sequentially fed, wide bandwidth, circularly polarised microstrip antennas," *Proc. IEEE*, vol. 136, no. 5, pp. 381–389, Oct 1989.
- [8] "RO3000 series." [Online]. Available: [https://www.rogerscorp.com/Advanced Connectivity Solutions/RO3000 Series Laminates](https://www.rogerscorp.com/Advanced_Connectivity_Solutions/RO3000_Series_Laminates)